

# Efficient H<sub>2</sub>O<sub>2</sub> Oxidation of Organic Pollutants Catalyzed by Supported Iron Sulfophenylporphyrin under Visible Light Irradiation

Yingping Huang, Jing Li, Wanhong Ma, Mingming Cheng, and Jincai Zhao\*

Laboratory of Photochemistry, Center for Molecular Sciences, Institute of Chemistry, Chinese Academy of Sciences, Beijing 100080, China

Jimmy C. Yu

Department of Chemistry, The Chinese University of Hong Kong, Shatin, N.T., Hong Kong, China

Received: July 15, 2003; In Final Form: December 25, 2003

An efficient method has been developed to degrade toxic and nonbiodegradable organic pollutants such as Sulforhodamine B (SRB) and 2,4-dichlorophenol (DCP). It is based on the photocatalytic power of iron tetrasulfophenylporphyrin supported on a commercial anionic ion-exchange resin (Amberlite IRA 900) (FePR) to activate an oxidant H<sub>2</sub>O<sub>2</sub> in aqueous media. Visible light irradiation ( $\lambda > 450$  nm) significantly accelerates the degradation process. The new catalyst is effective over a wide pH range, and can be easily recycled by filtration. The SRB and DCP were mineralized with yields of 56% and 68% at a catalyst/substrate molar ratio of 1:33 and 1:535, respectively. Moreover, the supported-catalyst would suppress greatly the undesirable side-reaction of H<sub>2</sub>O<sub>2</sub> conversion to O<sub>2</sub>. UV-vis spectroscopy, high-performance liquid chromatography, ion chromatography, IR, spin-trapping electron paramagnetic resonance, surface photovoltage spectroscopy, and total organic carbon measurements were used to examine the photoreaction processes. The photocatalytic degradation pathways mainly involve the formation and reaction of  $\cdot$ OH radicals. On the basis of the experimental results, a possible reaction mechanism is proposed.

## Introduction

Degradation of persistent and nonbiodegradable organic pollutants by oxidation with H<sub>2</sub>O<sub>2</sub> has been studied extensively.<sup>1–4</sup> It has also been found that oxidants including HSO<sub>5</sub><sup>−</sup>,<sup>5</sup> O<sub>2</sub>,<sup>6</sup> and H<sub>2</sub>O<sub>2</sub><sup>7–10</sup> could be activated catalytically by metal complexes such as metalloporphyrin,<sup>10</sup> metallophthalocyanine,<sup>7,9</sup> and tetraamido macrocyclic ligand.<sup>8</sup> In fact, these metal complexes can mimic the action of natural enzymes such as peroxidase and P450 in activating H<sub>2</sub>O<sub>2</sub> and O<sub>2</sub> in aqueous media.<sup>11,12</sup> Despite their potential, these synthetic catalysts have a serious flaw. They have fewer binding sites than their natural enzyme counterparts, and thus exhibit lower catalytic activity and poorer stability than peroxidase and P450.<sup>13</sup> Two approaches for improvement have been proposed by using (1) a heterogeneous supported catalyst system, and (2) a homogeneous supramolecular metal complex system.<sup>14,15</sup> Appropriate support materials, such as neutral organic polymers, ion exchange membranes or resins, and inorganic materials (clay, zeolites, etc.), would provide binding sites that allow the catalytic oxidation reaction to occur more efficiently.<sup>16,17</sup> Another advantage of a supported catalyst system is the ease of separation from the reaction solution by filtration.<sup>18</sup> Meunier et al.<sup>19</sup> reported a novel system in which iron tetrasulfophthalocyanine (FePcS) supported on an anionic resin was used as catalyst to degrade chlorophenols in an acetonitrile/H<sub>2</sub>O solvent mixture using KHSO<sub>5</sub> as an oxidant. However, the relatively low catalytic activity and a need for an organic cosolvent render this method impractical for pollution treatment. Recently, preliminary results reported by our group in a communication<sup>20</sup>

show that the iron tetrasulfophthalocyanine (FePcS) supported on a resin can catalyze H<sub>2</sub>O<sub>2</sub> to degrade Orange-II and salicylic acid under visible irradiation without the addition of CH<sub>3</sub>CN. However, FePcS supported on the resin exhibits scarce photocatalytic activity for the degradation of some organic pollutants such as 2,4-dichlorophenol and also gives much low activity at neutral pH values. Clearly, there is a demand for new supported metal complexes that possess excellent catalytic activity, high stability, and ease of posttreatment separation.<sup>18</sup> Also, it is very important to further investigate the photocatalytic reaction mechanism for the degradation of organic pollutants in water using supported metal complexes as photocatalysts.

Herein, we describe the development of a new catalytic system consisting of iron tetrasulfophenylporphyrin supported on a commercial anionic ion-exchange resin (Amberlite IRA 900) (FePR). This system is highly effective in activating H<sub>2</sub>O<sub>2</sub> for the photooxidation of an organic dye (sulforhodamine B, SRB) and a small molecular compound (2,4-dichlorophenol, DCP) under visible light irradiation ( $\lambda > 450$  nm). The effectiveness of this system is compared with an analogous process involving a homogeneous FeTPPS<sub>4</sub> catalyst in solution. The results indicate that both organic dyes and small organic compounds can be effectively degraded under visible light irradiation. The mineralization yields of SRB and DCP are 56% and 68%, respectively. In particular, FePR shows 3.5 times higher activity for the degradation of SRB than FeTPPS<sub>4</sub> does under the otherwise identical experimental conditions. The stability of FePR is also much higher than that of FeTPPS<sub>4</sub> under the same illumination intensity. Interestingly, the FePR catalyst can actually inhibit the direct decomposition of H<sub>2</sub>O<sub>2</sub> to O<sub>2</sub> in the photocatalytic system. In addition, the supported catalyst

\* Author to whom correspondence should be addressed. Fax: (+86)-10-8261-6495. E-mail: jczhao@iccas.ac.cn.

FePR can be separated easily from the reaction system and be reused. It is a significant advantage in the environmental treatment of toxic nonbiodegradable organic pollutants.

### Experimental Section

**Materials.** Sulforhodamine B (SRB, Acros) (see the structure below), Organe II (Acros), 2,4-dichlorophenol (DCP), and H<sub>2</sub>O<sub>2</sub> were of analytical reagent grade and were used without further purification. 5,5-Dimethyl-1-pyrroline-*N*-oxide (DMPO, Sigma) was used as the ESR spin-trapping reagent. Tetraphenylporphine tetrasulfonic acid (TPPS<sub>4</sub>) was purchased from Tokyo Kasei Kogyo Co., Ltd. The anionic exchange resin containing ammonium groups (macroreticular resin of moderately high porosity with benzyltrialkylammonium functionality, Amberlite IRA-900) was obtained from Aldrich. Horseradish peroxidase (POD) was purchased from Humei Biologic Engineering Co., and *N,N*-dimethyl-*p*-phenylenediamine (DPD) reagent was purchased from Merck. NaOH and HClO<sub>4</sub> solutions were used to adjust the pH of the solution. Deionized and doubly distilled water was used throughout this study. FeTPPS<sub>4</sub> was prepared by dissolving 40 mg of TPPS<sub>4</sub> and 10 mL of 4.3 × 10<sup>-3</sup> mol/L Fe(ClO<sub>4</sub>)<sub>3</sub> with 10 mL of water into a rockered flask. The solution was held at 100 °C with reflux for 10 h until the Sort band of TPPS<sub>4</sub> (420 nm) disappeared and characteristic band of FeTPPS<sub>4</sub> (380 nm) appeared. Excessive Fe<sup>3+</sup> was eliminated by cationic ion-exchange resin (Amberlite IR-120B). The Amberlite IRA 900 resin, after being ground and sieved by 200 meshes, was pretreated by alcohol, HCl, NaOH solution, and water in turn to remove the impurities. FePR with different exchange quantities were prepared by the addition of 500 mg of the pretreated Amberlite IR A 900 to an aqueous solution of FeTPPS<sub>4</sub> at different concentrations after 24 h of gentle magnetic stirring. The exchange amount of FeTPPS<sub>4</sub> onto resin also was calculated by measuring the concentration of FeTPPS<sub>4</sub> in the solution by a spectrophotometric method. The FePR catalyst with a different exchange amount of FeTPPS<sub>4</sub> onto resin was separated by filtration, and washed with water until no FeTPPS<sub>4</sub> could be detected in the washing solution. The catalysts were dried in air at room temperature and then at 65 °C for 48 h. The amount of saturated exchange for FeTPPS<sub>4</sub> by 1 g of resin is 33 μmol. The catalysts with exchange amounts of 33, 15, and 8 μmol/g of resin, respectively, were prepared. The FePR catalyst of 15 μmol/g resin exchange amount exhibited the highest activity compared to the other two catalysts with different exchange amounts, and therefore was used for all experiments.

**Photoreactor and Light Source.** A 500-W halogen lamp (Institute of Electric Light Source, Beijing) used as the visible light source was positioned inside a cylindrical Pyrex vessel surrounded by a jacket with circulating water (Pyrex) to cool the lamp. A cutoff filter (diameter = 3 cm) was used to completely remove wavelengths less than 450 nm and to ensure irradiation only by visible light ( $\lambda > 450$  nm). The distance between the reaction vessel and light source was 10 cm.

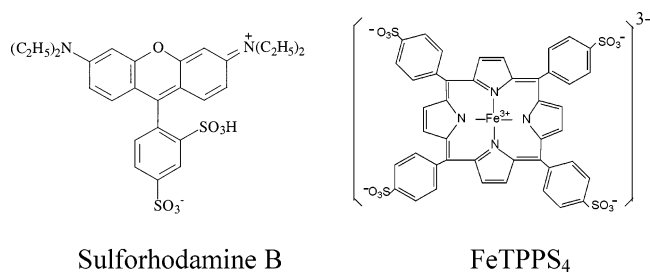
**Procedures and Analyses.** Unless otherwise noted, all the experiments were carried out in a Pyrex vessel (60 mL) in aerated solutions. At given irradiation time intervals, 3-mL samples were collected and analyzed immediately by observation of variations in the UV/vis spectra using a Hitachi 3010 spectrophotometer. Also, UV-vis diffuse reflectance spectra of the FePR and resin blank were determined using the Hitachi 3010 spectrophotometer equipped with integrator ( $\Phi$  150 mm). The amounts of SO<sub>4</sub><sup>2-</sup> and Cl<sup>-</sup> ions were analyzed by a DX-120 ion chromatograph (DIONEX) using an eluent of NaOH

(10 mM), and an eluent composed of Na<sub>2</sub>CO<sub>3</sub> (1.8 mM) and NaHCO<sub>3</sub> (1.7 mM), respectively. The photodegradation of DCP (no absorption in the visible region) was analyzed by high-performance liquid chromatography (HPLC) on an inersil ODS-3 5-μm column (250 × 4.6 mm) at room temperature. The HPLC system consisted of a Dionex P580 pump and a built-in UVD 340S diode array detector. DCP was detected at 304 nm by using an eluent composed of methanol/water (70%/30% v/v) at a flow rate of 1.0 mL/min. An Apollo 9000 TOC instrument was used for measurements of total organic carbon (TOC) values of the degraded solutions. The concentration of H<sub>2</sub>O<sub>2</sub> was measured by the POD method in which the DPD is oxidized by H<sub>2</sub>O<sub>2</sub> based on the POD-catalyzed reaction ( $\epsilon = 2.1 \times 10^4 \text{ M}^{-1} \text{ cm}^{-1}$ ).<sup>21</sup> The concentrations of Fe<sup>2+</sup> or Fe<sup>3+</sup> after reduction by hydroxylammonium chloride were measured spectrophotometrically by a 1,10-phenanthroline method with a detection limit of 1.8 × 10<sup>-7</sup> mol/L for Fe<sup>2+</sup> ( $\epsilon = 1.1 \times 10^4 \text{ M}^{-1} \text{ cm}^{-1}$ ).<sup>22</sup>

Surface photovoltage spectroscopy of photocatalysts was measured by surface photovoltage Stanford research systems equipped with a model SR 830 DSP lock-in amplifier. Infrared analysis was carried out with a TENSOR 27 (Bruker) FTIR spectrophotometer. The samples for the photodegradation of SRB were prepared as follows. The reacted solution was filtered, and the filtrate was evaporated (temperature below 323 K) under reduced pressure until water was mostly removed. Finally, the dried samples were further kept in a vessel containing P<sub>2</sub>O<sub>5</sub> for more than 24 h. The samples for IR were supported on anhydrous KBr. A Bruker model EPR 300E spectrometer equipped with a Quanta-Ray Nd:YAG laser (355 and 532 nm) was used for measurements of the electron paramagnetic resonance (EPR) signals of radicals spin-trapped by DMPO. The settings were the following: center field = 3486.7 G, sweep width = 100.0 G, microwave frequency = 9.82 GHz, and power = 5.05 mW. To minimize experimental errors, the same quartz capillary tube was used for all EPR measurements. A Trio-2000 model gas chromatography/mass spectroscopy (GC/MS) equipped with a BPX5 column, size 30 m × 0.25 mm, was used to analyze the photocatalytic reaction intermediates. Samples were prepared as follows: several dispersions (40 mL) containing SRB (1.25 × 10<sup>-4</sup> M), FePR (10 mg, 15 μmol FeTPPS<sub>4</sub> per gram of catalyst), were prepared. The absorption/desorption equilibrium was established between SRB and the resin with stirring for about 8 h. After H<sub>2</sub>O<sub>2</sub> (1.0 × 10<sup>-2</sup> M) was added, samples were irradiated with visible light at different time intervals. Then, the supported catalyst (FePR) was removed by filtration. Subsequently, the water in the filtrate was removed under reduced pressure (below 60 °C). The remaining residue was dissolved in methanol.

For reference, the structures of SRB and FeTPPS<sub>4</sub> are shown below:

**CHART 1: Structures of Sulforhodamine B and FeTPPS<sub>4</sub>**



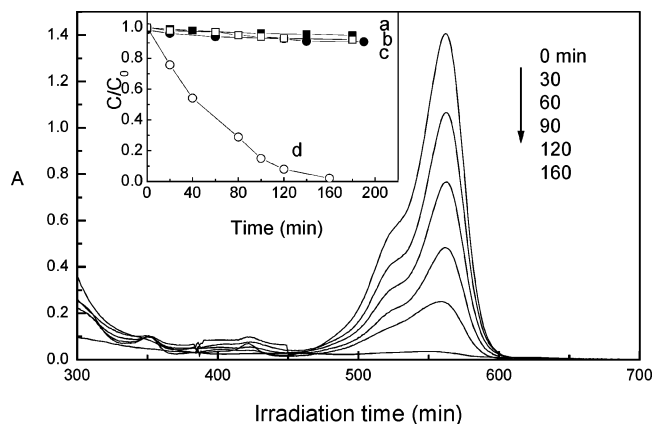


**Figure 1.** The degradation of SRB under different conditions: (a) SRB/FePR, visible light; (b) SRB/H<sub>2</sub>O<sub>2</sub>/FePR, in the dark; (c) SRB/H<sub>2</sub>O<sub>2</sub>, visible light; (d) SRB/H<sub>2</sub>O<sub>2</sub>/FePR, visible light. The reactions a–d were done at pH 9.0; [SRB] =  $1.25 \times 10^{-4}$  M; [FePR] = 10 mg/40 mL (15  $\mu$ mol FeTPPS<sub>4</sub>/g resin); [H<sub>2</sub>O<sub>2</sub>] =  $1.0 \times 10^{-2}$  M. The light intensity was 48 mW/cm<sup>2</sup>.

## Results and Discussion

**Photodegradation of Organic Compounds.** SRB and DCP were employed as model pollutants to examine their degradation and materialization with FePR as catalyst and H<sub>2</sub>O<sub>2</sub> as oxidant under visible irradiation ( $\lambda > 450$  nm). The photodegradation of organic compounds was carried out after the adsorption/desorption equilibrium had been established between the resin and organic compounds. During the degradation of SRB, the characteristic absorption peak of SRB at 565 nm in UV–vis spectra diminished and disappeared completely after visible irradiation for 160 min (Figure 1). The degradation rates of SRB with and without visible irradiation are shown in the inset of Figure 1.

In the absence of FePR (curve c) or H<sub>2</sub>O<sub>2</sub> (curve a), the degradation of SRB was scarcely observable under the visible irradiation. No obvious degradation of SRB was found in the dark (curve b). However, very significant degradation of SRB occurred under visible irradiation for the SRB/FePR/H<sub>2</sub>O<sub>2</sub> system (curve d). It indicated that visible irradiation and the presence of both photocatalyst and H<sub>2</sub>O<sub>2</sub> are necessary for the degradation reaction of substrates. The first-order kinetic constant of the photodegradation of SRB for SRB/FePR/H<sub>2</sub>O<sub>2</sub> was obtained ( $k_{hv} = 1.3 \times 10^{-2} \text{ min}^{-1}$ ). However, under the otherwise identical experimental conditions,  $k_{hv}$  was  $4.3 \times 10^{-3} \text{ min}^{-1}$  for the SRB/FeTPPS<sub>4</sub>/H<sub>2</sub>O<sub>2</sub> system. FePR exhibited higher catalytic activity than FeTPPS<sub>4</sub>. During the photocatalytic degradation of SRB in the FePR/H<sub>2</sub>O<sub>2</sub> system, the catalyst surface before irradiation was red-brown in color, due to the adsorption of SRB. After exposure to visible irradiation for about 160 min, the surface of the catalyst renewed to the blue (inherent color of FePR). This suggests that the substrate molecules both on the surface of the support catalyst and in the bulk solution can be efficiently degraded, and the catalyst is stable for the photocatalytic degradation of organic compounds with H<sub>2</sub>O<sub>2</sub> as oxidant. Meanwhile, no free Fe<sup>2+</sup> or Fe<sup>3+</sup> and FeTPPS<sub>4</sub> were detected in the degraded solution using the spectrophotometric method.<sup>22</sup>

Under similar experimental conditions, the photodegradation of DCP under visible irradiation was monitored by HPLC using an eluent of methanol/water (70%:30%) with ultraviolet detection at 304 nm; the degradation kinetics of DCP is displayed in Figure 2. The degradation of DCP hardly took place both in the dark (curve c) and in the presence of H<sub>2</sub>O<sub>2</sub> alone (curve b)

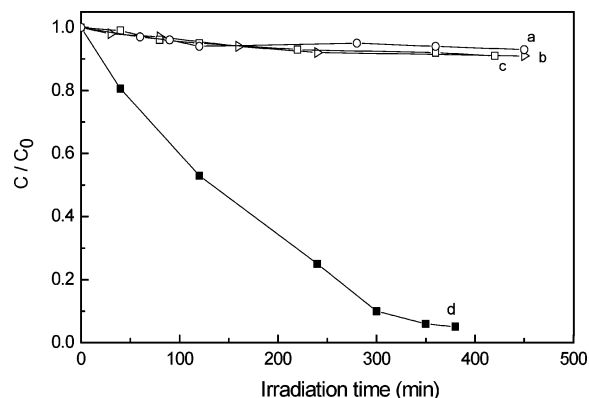


**Figure 2.** Photodegradation of DCP under different conditions: (a) DCP/FePR, visible light; (b) DCP/H<sub>2</sub>O<sub>2</sub>, visible light; (c) DCP/H<sub>2</sub>O<sub>2</sub>/FePR, dark; (d) DCP/H<sub>2</sub>O<sub>2</sub>/FePR, visible light. Reactions a–d were done at pH 9.0; [DCP] =  $1.0 \times 10^{-3}$  M; [FePR] = 5 mg/40 mL (15  $\mu$ mol FeTPPS<sub>4</sub> per g resin); [H<sub>2</sub>O<sub>2</sub>] =  $4.0 \times 10^{-2}$  M. The light intensity was 48 mW/cm<sup>2</sup>.

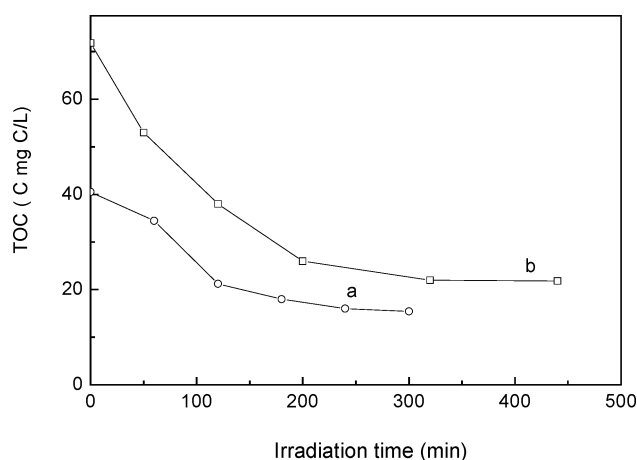


**Figure 3.** TOC removal of SRB (curve a, [SRB] =  $1.25 \times 10^{-4}$  M, [H<sub>2</sub>O<sub>2</sub>] =  $2.0 \times 10^{-2}$  M) and DCP (curve b, [DCP] =  $1.0 \times 10^{-3}$  M, [H<sub>2</sub>O<sub>2</sub>] =  $4.0 \times 10^{-2}$  M) in the presence of FePR/H<sub>2</sub>O<sub>2</sub> as a function of irradiation time. Initial conditions: The amount of FePR: 10 mg for SRB, 5 mg for DCP; V = 40 mL; pH 9.2.

or FePR alone (curve a) under visible irradiation. Visible irradiation could effectively accelerate the degradation reaction of DCP in the DCP/FePR/H<sub>2</sub>O<sub>2</sub> system (curve d). This rapid degradation of DCP that has no absorption above a wavelength of 310 nm illustrates that the photoexcitation of FePR by visible light initiates the photocatalytic degradation process and the photosensitization process induced by the photoexcitation of substrates does not play a major role.

The mineralization degree of the organic compounds was evaluated by determination of the changes in the total organic carbon (TOC) in the photodegradation of SRB and DCP. After the photocatalytic reaction proceeded for 300 min and 450 min for SRB and DCP in the presence of FePR and H<sub>2</sub>O<sub>2</sub> under visible irradiation, the TOC removal yields for SRB and DCP were 56% and 68%, respectively (seen Figure 3).

The free SO<sub>4</sub><sup>2-</sup> and Cl<sup>-</sup> ions were also determined in the degradation of SRB and DCP, respectively, under visible irradiation by an ion chromatograph (see Figure 4). About 65% of the SO<sub>4</sub><sup>2-</sup> free ion from SRB and 70% of the Cl<sup>-</sup> ion from DCP were released in the reaction solution after 160 min and 380 min of photocatalytic reaction SRB and DCP of in the presence of FePR and H<sub>2</sub>O<sub>2</sub> under visible irradiation, respectively. These results indicate that both SRB and DCP underwent

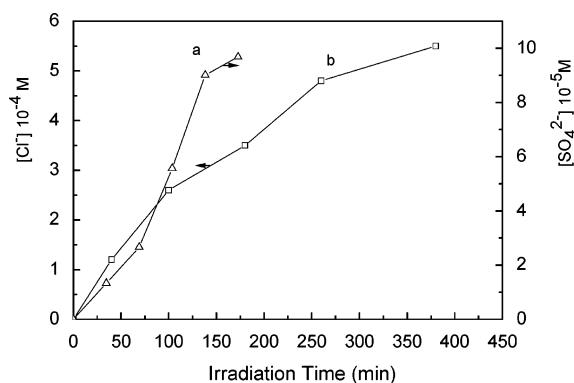


**Figure 4.** Evolution of  $\text{SO}_4^{2-}$  (curve a) and  $\text{Cl}^-$  ions (curve b) during the photodegradation of SRB and DCP, respectively. For curve a,  $[\text{SRB}] = 7.5 \times 10^{-5} \text{ M}$ ;  $[\text{FePR}] = 10 \text{ mg}/40 \text{ mL}$  ( $15 \mu\text{mol FeTPPS}_4$  per 1 g resin);  $[\text{H}_2\text{O}_2] = 1.0 \times 10^{-2} \text{ M}$ . pH = 9.0, for curve b,  $[\text{DCP}] = 4.0 \times 10^{-4} \text{ M}$ ;  $[\text{FePR}] = 5 \text{ mg}/40 \text{ mL}$  ( $15 \mu\text{mol FeTPPS}_4$  per 1 g resin);  $[\text{H}_2\text{O}_2] = 4.0 \times 10^{-2} \text{ M}$ ; pH = 9.2.

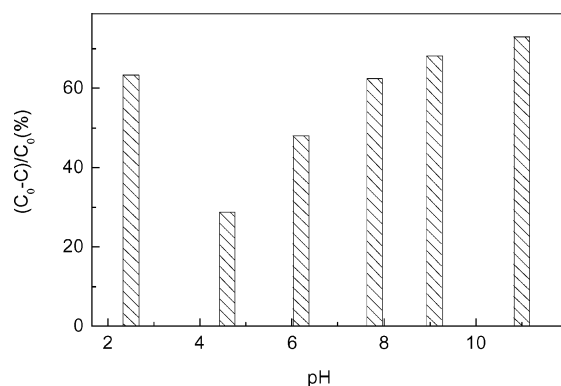


**Figure 5.** Effect of pH on the degradation of SRB ( $1.25 \times 10^{-4} \text{ M}$ ) in the presence of FePR (10 mg/40 mL) and  $\text{H}_2\text{O}_2$  ( $1.0 \times 10^{-2} \text{ M}$ ) under visible irradiation.

not only a simple discoloration or dechlorination but also an irreversible decomposition in the photocatalytic reaction.

In addition, FePR as catalyst can also efficiently degrade the others anionic compounds, such as Orange-II ( $[\text{Orange-II}] = 1.25 \times 10^{-4} \text{ M}$ ,  $[\text{FePR}] = 10 \text{ mg}/40 \text{ mL}$ ,  $[\text{H}_2\text{O}_2] = 5.5 \times 10^{-4} \text{ M}$ , pH = 9.2, the first-order kinetic constant was  $1.2 \times 10^{-2} \text{ min}^{-1}$ ), salicylic acid (SA) ( $[\text{SA}] = 1.2 \times 10^{-3} \text{ M}$ ,  $[\text{FePR}] = 5 \text{ mg}/40 \text{ mL}$ ,  $[\text{H}_2\text{O}_2] = 2 \times 10^{-2} \text{ M}$ , pH = 9.0, the first-order kinetic constant was  $6.2 \times 10^{-3} \text{ min}^{-1}$ ). Because of the properties of the resin, which can easily adsorb anionic compounds, types of the cationic compounds such as Rhodamine B (RhB) and Malachite Green (MG) were found not obviously degraded under the same experimental conditions, because they are hardly adsorbed on the catalyst. However,  $\text{FeTPPS}_4$  in the solution can degrade both the cationic and anionic compounds such as RhB, MG, SRB, and orange-II with  $\text{H}_2\text{O}_2$  as oxidant under visible irradiation, indicating that FePR is a kind of selective photocatalyst for the degradation of anionic and nonionic compounds.

FePR catalyst at a wide pH range from 1 to 11.0 exhibits excellent catalytic activity for the degradation of SRB. The greatest degradation rates in 60 min of reaction were found at pH < 4.0 and pH > 7.8 (see Figure 5). FePR also has very high catalytic activity, even at natural pH values (pH 6–8). It seems that the optimal pH value depends on the both the adsorption property of substrate on the resin and the catalytic activity of the catalyst. The  $\text{FeTPPS}_4$  in solution has better catalytic activity only at pH > 11.0 for the degradation of SRB.

More interesting was the behavior of  $\text{H}_2\text{O}_2$  decomposition

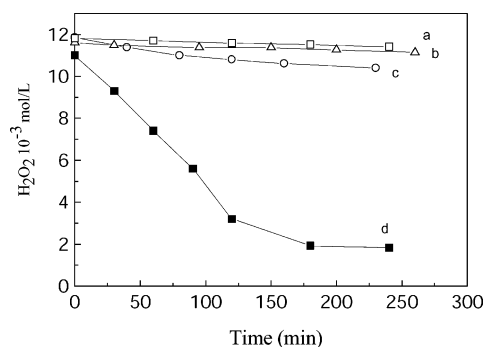


**Figure 6.** Decomposition of  $\text{H}_2\text{O}_2$  for the SRB/FePR system under visible light irradiation. Initial:  $[\text{SRB}] = 2.0 \times 10^{-4} \text{ M}$  40 mL;  $[\text{H}_2\text{O}_2] = 1.2 \times 10^{-2} \text{ M}$ ;  $[\text{FePR}] = 10 \text{ mg}/40 \text{ mL}$ ; pH = 9.1. (a)  $\text{H}_2\text{O}_2/\text{FePR}$ , visible light; (b) SRB/ $\text{H}_2\text{O}_2$ , visible light, (c) SRB/ $\text{H}_2\text{O}_2/\text{FePR}$  in the dark; (d) SRB/ $\text{H}_2\text{O}_2/\text{FePR}$ , visible light.

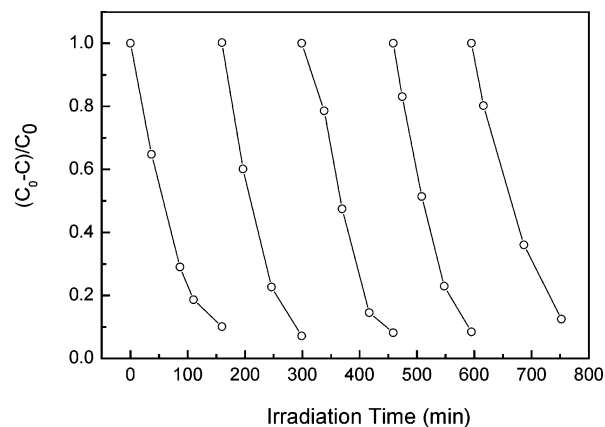


**Figure 7.** Catalyst recycling in repetitive degradation of SRB ( $1.25 \times 10^{-4} \text{ M}/\text{run}$ ) by  $\text{H}_2\text{O}_2$  ( $1.0 \times 10^{-2} \text{ M}$ ) in the presence of FePR (10 mg/40 mL).

during the photocatalytic degradation of substrates using FePR as catalyst under visible irradiation. The decomposition of  $\text{H}_2\text{O}_2$  relies on degradation of substrates (see Figure 6). No  $\text{H}_2\text{O}_2$  decomposition was observed either when the SRB was absent under visible irradiation in the presence of catalyst or when the reaction was performed in the dark in the presence of both substrates and catalyst. This is significantly different from the homogeneous photoreaction catalyzed by  $\text{FeTPPS}_4$  (or  $\text{Fe}^{3+}/\text{Fe}^{2+}$ ) in which  $\text{H}_2\text{O}_2$  suffers rapid decomposition regardless of the organic substrates. This rigorous correlation suggests that present system provides a more economical  $\text{H}_2\text{O}_2$  usage for the photooxidation of organic pollutants.

The FePR as a kind of heterogeneous photocatalyst can be easily recycled by a simple filtration. After 5 recycles for the photodegradation of SRB (0.125 mM SRB/each cycle, 10 mg catalyst/40 mL), the catalyst did not exhibit any significant loss of activity (seen Figure 7). Confirming that the  $\text{FeTPPS}_4$  supported on the resin cannot be obviously degraded during the photocatalytic oxidation of the pollutant molecules. However, the  $\text{FeTPPS}_4$  in homogeneous solution was not stable using  $\text{H}_2\text{O}_2$  as oxidant under visible irradiation. The catalytic activity of  $\text{FeTPPS}_4$  in the solution in the second cycle was about 40% of that of the first run. In addition, no  $\text{Fe}^{2+}$  or  $\text{Fe}^{3+}$  ions as well as  $\text{FeTPPS}_4$  in the reaction bulk solution were detected using the spectrophotometric method<sup>22</sup> for FePR/SRB/ $\text{H}_2\text{O}_2$  system. An important advantage of this photocatalyst is that the photocatalyst can be removed easily from the reaction solution by simple filtrates and reused for the photocatalytic experiments without significant loss of activity.

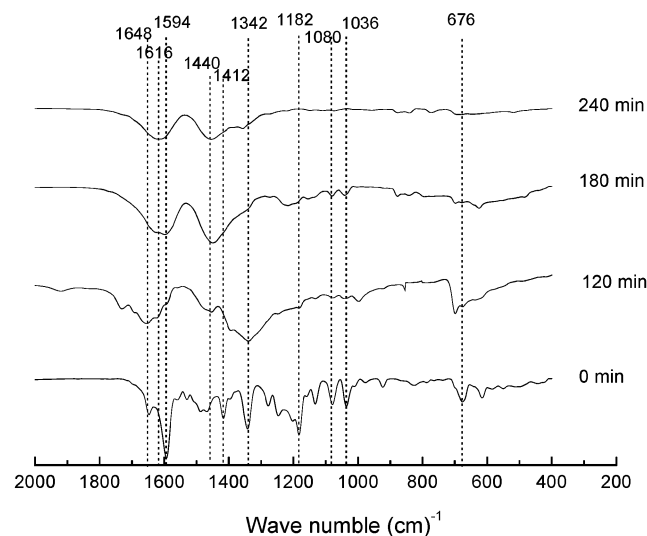


**Figure 8.** IR spectrum of the intermediates during the degradation of SRB ( $1.25 \times 10^{-4}$  M) in H<sub>2</sub>O<sub>2</sub> ( $1.0 \times 10^{-2}$  M)/FePR (10 mg/40 mL) system under visible light irradiation at pH 9.0.

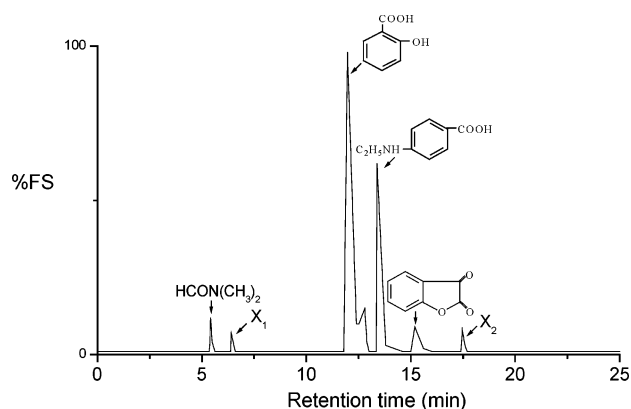


**Figure 9.** GC spectra of the degradation products formed in the visible light-assisted photodegradation of SRB in the presence of FePR and H<sub>2</sub>O<sub>2</sub> with retention time. Column: BPX5, 30 m  $\times$  0.25 mm.

**Analysis of the Intermediates in the Photocatalytic Degradation of SRB.** The IR spectroscopy was used to monitor the temporal course of the photodegradation conversion of SRB (Figure 8).

Before irradiation, the band at 1594 cm<sup>-1</sup> corresponds to aromatic ring vibrations, whereas the 1342 cm<sup>-1</sup> band is due to C-aryl bond vibrations. The bands at 1182 cm<sup>-1</sup> and 676 cm<sup>-1</sup> are caused by vibrations of the -SO<sub>3</sub> groups. The band

at 1648 cm<sup>-1</sup> is attributed to vibrations of the carbon-nitrogen bond.<sup>23</sup> As the photocatalytic reaction preceded, bands of characteristic vibrations of the carbon-nitrogen bond (1648 cm<sup>-1</sup>), the C-aryl bond (1342 cm<sup>-1</sup>), and the aromatic ring (1594 cm<sup>-1</sup>) decreased with the irradiation time and disappeared after about 4 h of photoreaction. In addition, bands of the -SO<sub>3</sub> group (1182 cm<sup>-1</sup>, 676 cm<sup>-1</sup>) also completely disappeared. With the photocatalytic reaction process, two strong new IR bonds at 1440 cm<sup>-1</sup> and 1616 cm<sup>-1</sup> attributable to carboxylic acid and primary amines intermediates appeared.<sup>24</sup> The IR results indicate that the large conjugated chromophore structure of SRB was destroyed and further decomposed to smaller organic species under visible irradiation.

The GC-MS results of the photooxidation intermediates for SRB/FePR/H<sub>2</sub>O<sub>2</sub> system are presented in Figure 9.

The results of gas chromatography in Figure 9 show that obviously six different peaks appeared. Among the intermediates, *N,N*-dimethylformamide (A), 2-hydroxybenzoic acid (B), 4-(ethylamino)benzoic acid (C), and 1,3-isobenzofurandione (D), respectively, were identified. These products of mainly small organic acids and amines are all biodegradable. No signals of SRB in the products were observed for the photodegradation of SRB in the absence of H<sub>2</sub>O<sub>2</sub> under the same experimental conditions as above or in the presence of FePR and H<sub>2</sub>O<sub>2</sub> in the dark.

The information about active radicals involved for the photodegradation of SRB with H<sub>2</sub>O<sub>2</sub> as oxidant and FePR as catalyst was obtained using spin-trapping ESR (Figure 10). No ESR signals were observed either when the organic substrate was absent under visible irradiation in the presence of catalyst, or when the reaction was performed in the dark for the aqueous SRB/FePR/H<sub>2</sub>O<sub>2</sub> system. Under visible irradiation the characteristic quartet peaks of DMPO-<sup>•</sup>OH adducts appeared gradually in the aqueous SRB/FePR/H<sub>2</sub>O<sub>2</sub> system, and the intensity increased with irradiation time. The ESR signals of DMPO-<sup>•</sup>OOH/O<sub>2</sub><sup>-•</sup> adducts with characteristic six peaks were observed under visible irradiation in the methanol media, since the <sup>•</sup>OOH/O<sub>2</sub><sup>-•</sup> radicals are very unstable and undergo facile disproportionation rather than slow reaction with DMPO in aqueous solution, and the <sup>•</sup>OOH/O<sub>2</sub><sup>-•</sup> radicals can be trapped by DMPO and detected in the organic media such as CH<sub>3</sub>OH even containing a part of water.<sup>25</sup> However, the intensity is much weaker (see Figure 10), and its intensity scarcely increased with irradiation time. It indicated that photocatalytic reaction for SRB/FePR/H<sub>2</sub>O<sub>2</sub> mainly involved the <sup>•</sup>OH radical. For comparison, the ESR also was measured for the homogeneous SRB/FeTPPS<sub>4</sub>/H<sub>2</sub>O<sub>2</sub> system. The signals of DMPO-<sup>•</sup>OH adducts increased with irradiation time (Figure 12).

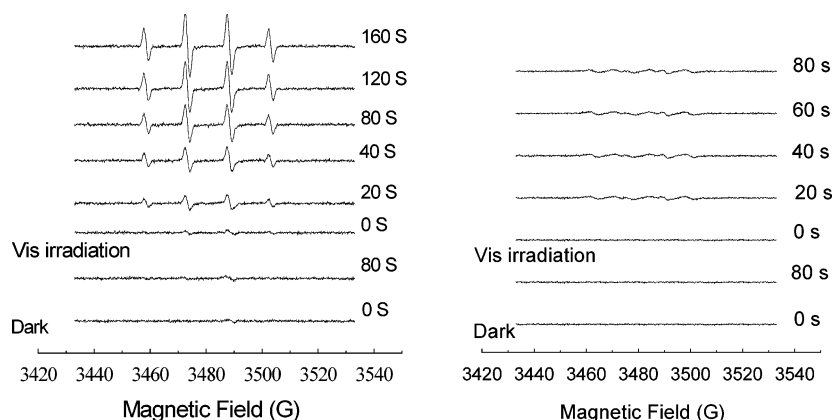


**Figure 10.** The ESR signals of the DMPO-<sup>•</sup>OH (left, aqueous solution) and DMPO-<sup>•</sup>OOH (right, methanol media) adducts for SRB/FePR/H<sub>2</sub>O<sub>2</sub> system in the dark and under visible irradiation [FePR] = 5 mg/40 mL; [SRB] =  $1.25 \times 10^{-4}$  M; [H<sub>2</sub>O<sub>2</sub>] =  $1.0 \times 10^{-2}$  M; [DMPO] = 0.04 M.

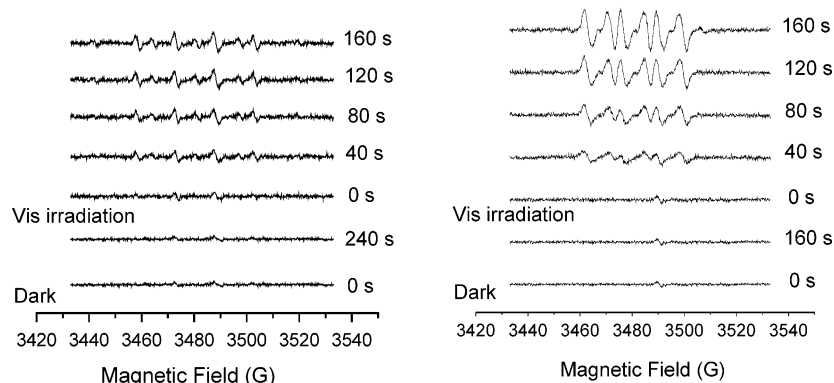


**Figure 11.** The ESR signals of the DMPO- $\cdot$ OH (left, aqueous solution) and DMPO- $\cdot$ OOH (right, methanol media) adducts for SRB/FeTPPS<sub>4</sub>/H<sub>2</sub>O<sub>2</sub> system in the dark and under visible irradiation [FeTPPS<sub>4</sub>] =  $1.87 \times 10^{-6}$  M; [SRB] =  $1.25 \times 10^{-4}$  M; [H<sub>2</sub>O<sub>2</sub>] =  $1.0 \times 10^{-2}$  M; [DMPO] = 0.04 M.

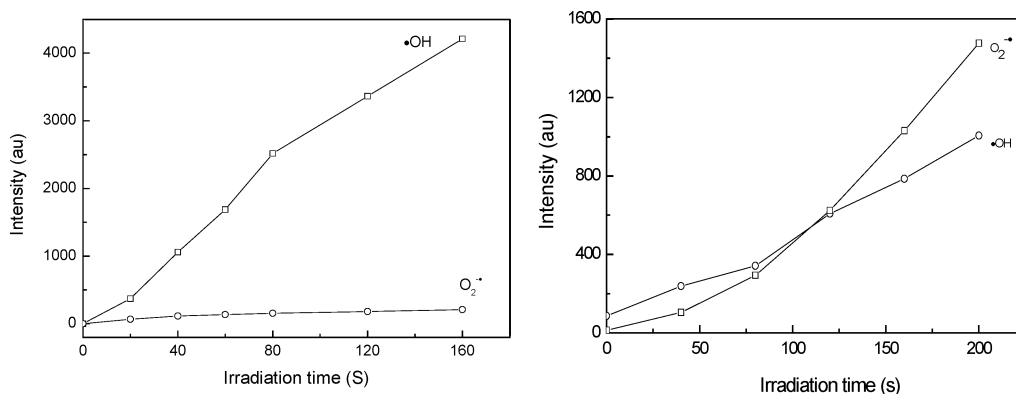
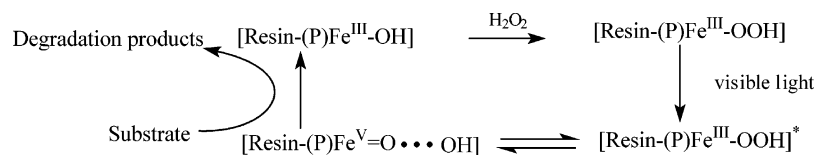


**Figure 12.** Comparison of radical intensity of  $\cdot$ OH and  $O_2^{\cdot-}$  for the SRB/FePR/H<sub>2</sub>O<sub>2</sub> system (left) and the SRB/FeTPPS<sub>4</sub>/H<sub>2</sub>O<sub>2</sub> system (right) irradiated by laser ( $\lambda = 532$  nm). Conditions: [FePR] = 5 mg/40 mL; [SRB] =  $1.25 \times 10^{-4}$  M; [H<sub>2</sub>O<sub>2</sub>] =  $1.0 \times 10^{-2}$  M; [DMPO] = 0.04 M; [FeTPPS<sub>4</sub>] =  $1.87 \times 10^{-6}$  M.

### SCHEME 1: Proposed Photodegradation Mechanism of Organic Pollutants in the Aqueous H<sub>2</sub>O<sub>2</sub>/FePR System under Visible Light Irradiation



Under the same experiment conditions, the intensity of  $\cdot$ OH radicals was less than that of the FePR system. The intensity of  $\cdot$ OOH/ $O_2^{\cdot-}$  obviously increased with irradiation time for the FeTPPS<sub>4</sub> system (Figure 11). The relative intensity for  $\cdot$ OH and  $\cdot$ OOH/ $O_2^{\cdot-}$  is displayed in Figure 12. Because  $\cdot$ OOH/ $O_2^{\cdot-}$  radicals in aqueous solution can easily undergo further disproportionation into  $O_2$  that is a side-reaction of H<sub>2</sub>O<sub>2</sub>, we can find from Figure 12 that the supported-FeTPPS<sub>4</sub> photocatalyst utilizes H<sub>2</sub>O<sub>2</sub> more economically than the homogeneous FeTPPS<sub>4</sub> system. EPR signals were also measured for the DCP/FePR/H<sub>2</sub>O<sub>2</sub> system with 532 nm laser irradiation. The EPR signal intensity of the DMPO- $\cdot$ OH adducts was enhanced gradually with increasing illumination time. The case is the same as that for the FePR/SRB/H<sub>2</sub>O<sub>2</sub> system under our experimental conditions. No signals of DMPO- $\cdot$ OH adducts were observed in the dark under otherwise identical conditions as those in the photoreaction. It further clarifies that the degradation of organic compounds is derived mainly by the excitation of catalyst by visible light irradiation for supported catalyst systems.

On the basis of the experimental results and literature information, a possible photocatalytic reaction pathway for the degradation of organic compounds with FePR as catalyst and

H<sub>2</sub>O<sub>2</sub> as oxidant under visible irradiation is proposed as shown in Scheme 1.

First of all, [Fe<sup>III</sup>PR] forms [HOFe<sup>III</sup>PR] complex in aqueous solution.<sup>26</sup> Then, H<sub>2</sub>O<sub>2</sub> as nucleophilic addition reagent complexes to the axial site of the iron center of the [HOFePR] to give [HOFe<sup>III</sup>PR] species.<sup>27</sup> Upon visible irradiation, [HOFe<sup>III</sup>PR] is converted to [HOFe<sup>III</sup>PR]\* excited-state transition species,<sup>28</sup> which may undergo intramolecular electron transfer to generate [Fe<sup>II</sup>PR] and  $\cdot$ OOH intermediates.<sup>29</sup> However, this reaction is not significant in our system as evidenced by ESR experiments. Alternatively, the O-O band cleavage of [HOFe<sup>III</sup>PR]\* results in generation of [PRFe<sup>Vb</sup>=O] and  $\cdot$ OH radicals species.<sup>30</sup> The HO $\cdot$  radicals are much more active than that of [PRFe<sup>V</sup>=O] species. So, the photodegradation reaction with HO $\cdot$  radicals is predominant in the organics/FePR/H<sub>2</sub>O<sub>2</sub> system under visible irradiation. To evidence this notion, the influence of addition of methanol, a known scavenger of  $\cdot$ OH radicals, on the degradation of SRB was investigated under visible light irradiation for the SRB/FePR/H<sub>2</sub>O<sub>2</sub> system. The results indicated that addition of methanol decreased significantly the degradation of SRB at various concentrations of methanol. It further suggested that active species for the photocatalytic degradation

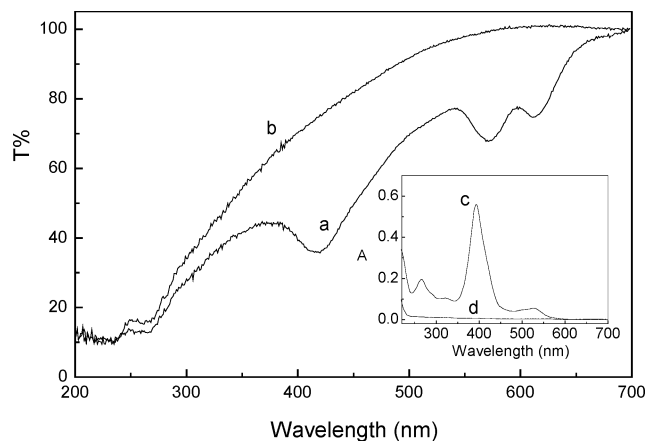


**Figure 13.** UV-vis diffuse reflectance spectra of FePR (curve a) and the blank resin (curve b). Inset: the absorption spectra of FeTPPS<sub>4</sub> (curve c) and Fe<sup>3+</sup> (curve d) in aqueous solution at pH = 9.0 and pH = 2.6, respectively. [FeTPPS<sub>4</sub>] = 1.0 × 10<sup>-6</sup> M, [Fe<sup>3+</sup>] = 4.3 × 10<sup>-3</sup> M.

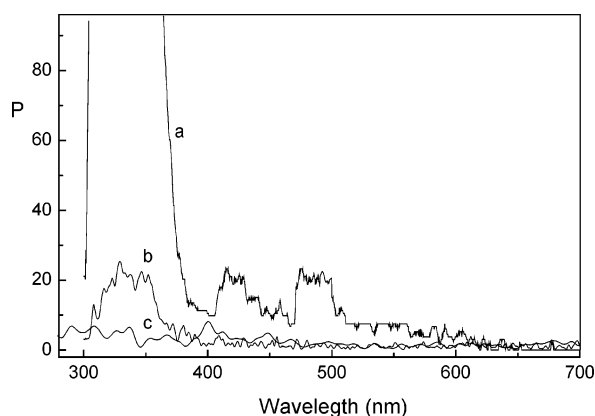


**Figure 14.** Surface photovoltage spectroscopy of FePR (curve a), FeTPPS<sub>4</sub> (curve b), and Fe<sup>3+</sup>-resin blank (curve c).

by FePR mainly are •OH radicals. HO• radicals generated will react immediately with organic pollutants and degrade them effectively. Without organic pollutants in the [FePR]/H<sub>2</sub>O<sub>2</sub> system, the HO• radicals would rapidly recombine with the [PRFe<sup>V</sup>=O] to renew H<sub>2</sub>O<sub>2</sub>. The detailed reaction mechanism needs further study.

**Photochemical Characteristics of FePR.** Figure 13 presents the UV-vis diffuse reflectance spectra of the FePR (curve a) and the blank resin (curve b). The absorption spectra of FeTPPS<sub>4</sub> (curve c) and Fe<sup>3+</sup> (curve d) in aqueous solution were also shown in the inset of Figure 13.

The maximum absorbance of FeTPPS<sub>4</sub> in aqueous solution was located at 383 nm and 525 nm. The FePR displays a very broad range absorbance in 200–700 nm regions with maxima located at 421 nm, 560 nm, and 620 nm. Such an extended coverage in the visible spectrum makes FePR possible to utilize most of the energy from sunlight. The difference in the absorption spectra between FePR and FeTPPS<sub>4</sub> also indicates the strong interaction between the sulfonate groups of the iron sulfoporphyrin and ammonium groups of the resin in the FePR catalyst.

Surface photovoltage spectroscopy (SPS) is also a useful method to evaluate illumination-induced charge transfer on the catalyst surface. The illumination-induced surface photovoltage spectra of FePR (curve a), FeTPPS<sub>4</sub> (curve b), and Fe<sup>3+</sup> resin blank (curve c) are displayed in Figure 14. It indicated that FePR could be excited much more effectively to cause charge transfer by visible irradiation ( $\lambda_{\max}$  421 nm and 480–520 nm) than

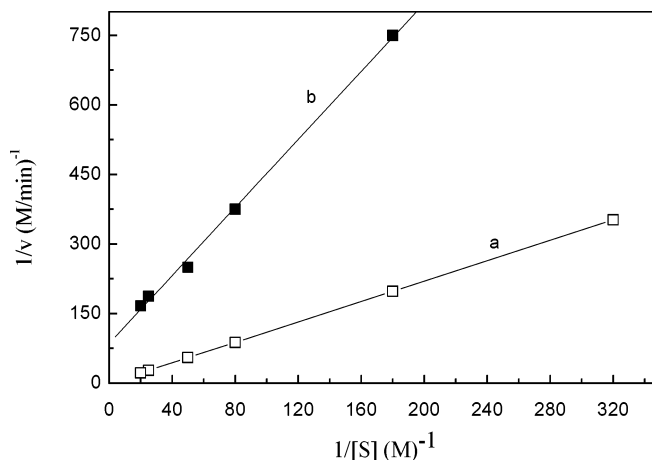


**Figure 15.** Relation between initial rate for the degradation of SRB (1.25 × 10<sup>-4</sup> M) with FePR (5 mg/40 mL) (a) or FeTPPS<sub>4</sub> (1.87 × 10<sup>-6</sup> M) (b) and the initial concentration of H<sub>2</sub>O<sub>2</sub>.

**TABLE 1: Catalytic Characteristics of FePR and FeTPPS<sub>4</sub> in Photodegradation of SRB with H<sub>2</sub>O<sub>2</sub> as Oxidant at pH = 9.0**

catalyst	$K_m$ (10 <sup>-3</sup> mol/L)	$V_{\max}$ (min)	[C] (10 <sup>-6</sup> M)	$K_{\text{cat}}$ (10 <sup>6</sup> M <sup>-1</sup> min <sup>-1</sup> )
FePR	19.14	0.99	1.87	0.53
FeTPPS <sub>4</sub>	9.28	0.27	1.82	0.15

FeTPPS<sub>4</sub>, or Fe<sup>3+</sup>-resin alone, suggesting that photochemistry properties of FePR are more advantageous than those of FeTPPS<sub>4</sub>.

We further compared the photodegradation of organic compounds (SRB) catalyzed by FePR and that by FeTPPS<sub>4</sub>. Photocatalytic reaction kinetic measurements (Figure 15) were made to reveal the relation between the degradation rate of SRB and the initial concentration of H<sub>2</sub>O<sub>2</sub> in the presence of FePR or FeTPPS<sub>4</sub>, respectively. The photodegradation rate of SRB increased with the increasing initial concentration of H<sub>2</sub>O<sub>2</sub> and then saturated. This phenomenon is similar to the enzyme catalytic reaction.<sup>31</sup> So, the kinetics of photodegradation of SRB with H<sub>2</sub>O<sub>2</sub> using FePR and FeTPPS<sub>4</sub> as catalysts were analyzed in a format similar to that used in enzymatic catalysis.

To set the experimental conditions, the initial concentrations of H<sub>2</sub>O<sub>2</sub> and SRB were kept in great excess over the concentration of the catalyst concentration. Then, the Michaelis–Menten equation is as follows:

$$\frac{1}{v} = \frac{1}{V_{\max}} \frac{1}{[S]} + \frac{1}{K_m}$$

where  $v$  represents velocity of degradation of SRB,  $[S]$  is the concentration of H<sub>2</sub>O<sub>2</sub>,  $K_m$  represents the affinity between the active site of catalyst and substrate,  $V_{\max}$  represents maximal catalytic reaction velocity of catalyst,  $K_{\text{cat}}$  is the catalytic constant of photocatalytic reaction, and  $K_{\text{cat}} = V_{\max}/[C]$ . Figure 15 shows the relation between the  $1/v$  and the  $1/[S]$ .

The results in Table 1 indicated that the activity of FePR is about 3.5 times that of FeTPPS<sub>4</sub> in aqueous solution for the photodegradation of SRB under visible irradiation. It proves that the supported catalyst exhibits excellent catalytic activity in the photocatalytic reaction process.

## Conclusion

Toxic and nonbiodegradable organic pollutants, such as Sulforhodamine B (SRB) and 2,4-dichlorophenol (DCP), can be efficiently photodegraded in an aqueous solution by using a

novel photocatalytic oxidation system consisting of H<sub>2</sub>O<sub>2</sub> and FeTPPS<sub>4</sub> supported on a resin. The FePR catalyst exhibits both much higher catalytic activity and much better stability than FeTPPS<sub>4</sub> in the homogeneous system for the photodegradation of organic pollutants, and the FePR can be recycled easily by filtration. It is interesting that the FePR catalyst can suppress the undesirable decomposition of H<sub>2</sub>O<sub>2</sub> to O<sub>2</sub>. This makes the FePR system more economical than the one with FeTPPS<sub>4</sub>. The reaction mechanism involves the formation and reaction of •OH radicals in the degradation pathways. This FePR/H<sub>2</sub>O<sub>2</sub> photocatalytic system provides new possibilities for the oxidative removal of persistent organic pollutants in aquatic environment under visible light irradiation.

**Acknowledgment.** The generous financial support by 973 project (No. 2003CB415006), the National Science Foundation of China (Grant No. 20133010, No. 20373074, No. 50221201, and No.20371048), the Chinese Academy of Sciences, Ministry of Science and Technology of China (No. 2002AA601250) is gratefully acknowledged.

### References and Notes

- (1) Walling, C. *Acc. Chem. Res.* **1975**, *8*, 125–131.
- (2) (a) Chen, F.; Ma, W. H.; He, J.; Zhao, J. C. *J. Phys. Chem. A* **2002**, *106*, 9485–9490. (b) Chen, F.; He, J.; Zhao, J. C.; Yu, J. C. *New J. Chem.* **2002**, *26*, 336–341.
- (3) Haeg, W. R.; Yao, C. D. *Environ. Sci. Technol.* **1992**, *26*, 1005–1009.
- (4) (a) Pignatello, J. J. *Environ. Sci. Technol.* **1992**, *26*, 944–951. (b) Chen, R.; Pignatello, J. J. *Environ. Sci. Technol.* **1997**, *31*, 2399–2406.
- (5) Meunier, B. *Chem. Rev.* **1992**, *92*, 1411–1456.
- (6) Ma, W.; Li, J.; Tao, X.; He, J.; Yu, J. C.; Zhao, J. C. *Angew. Chem., Int. Ed.* **2003**, *42*, 1029–1032.
- (7) (a) Sorokin, A.; Seris, J. L.; Meunier, B. *Science* **1995**, *268*, 1163–1166. (b) Labat, G.; Seris, J. L.; Meunier, B. *Angew. Chem., Int. Ed. Engl.* **1990**, *29* (12), 1471–1472.
- (8) (a) Collins, T. J. *Acc. Chem. Res.* **2002**, *35*, 782–790. (b) Miller, C. G.; Gordon-Wylie, S. W.; Horwitz, C. P.; Strazisar, S. A.; Per, D. K.; Clark, G. R.; Weintraub, S. T.; Collins, T. J. *J. Am. Chem. Soc.* **1998**, *120*, 11540–11541. (c) Gupta, S. S.; Stadler, M.; Noser, C. A.; Ghosh, A.; Steinhoff, B.; Lenoir, D.; Horwitz, C. P.; Schramm, K. W.; Collins, T. J. *Science* **2002**, *296* (12), 326–328.
- (9) (a) Tao, X.; Ma, W. H.; Zhang, T. Y.; Zhao, J. C. *Angew. Chem., Int. Ed.* **2001**, *40* (16), 3014–3016. (b) Tao, X.; Ma, W. H.; Zhang, T. Y.; Zhao, J. C. *Chem. Eur. J.* **2002**, *8* (6), 1321–1326.
- (10) Wariishi, H.; Kabuto, M.; Mikuni, J.; Oyadomari, M.; Tanaka, H. *Biotechnol. Prog.* **2002**, *18*, 36–42.
- (11) Solomn, E. I. *Inorg. Chem.* **2001**, *40*, 3656–3669. (b) Harris, D. L.; Loew, G. H. *J. Am. Chem. Soc.* **1998**, *120*, 8941–8948.
- (12) (a) Hollenberg, D. F.; Vaz, A. D.; Coon, M. J. *J. Am. Chem. Soc.* **2000**, *122* (12), 2677–2686. (b) Shearer, J.; Scarrow, R. C.; Kovacs, J. A. *J. Am. Chem. Soc.* **2002**, *124*, 11709–11717.
- (13) Que, L., Jr.; Ho, R. Y. N. *Chem. Rev.* **1996**, *96*, 2607–2624.
- (14) (a) Yang, R.; Li, K. A.; Wang, K. M.; Zhao, F. L.; Li, N.; Liu, F. *Anal. Chem.* **2003**, *75*, 612–621. (b) Kano, K.; Nishiyabu, R.; Asada, T.; Kuroda, Y. *J. Am. Chem. Soc.* **2002**, *124*, 9937–9944. (c) Gerrits, P. K.; Vos, D. D.; Starzyk, F. T.; Jacobs, P. A. *Nature* **1994**, *369* (16), 534–546.
- (15) Kakkar, A. *Chem. Rev.* **2002**, *102*, 3579–3588.
- (16) Nadochenko, V.; Kiwi, J. *Environ. Sci. Technol.* **1998**, *32*, 3282–3285.
- (17) Maldotti, A.; Molinari, A.; Amadellu, R. *Chem. Rev.* **2002**, *102*, 3811–3836.
- (18) Cole-hamilton, D. J. *Science* **2003**, *14*, 1702–17069.
- (19) Meunier, B.; Sorokin, A. *Acc. Chem. Res.* **1997**, *30*, 470–476.
- (20) Tao, X.; Ma, W. H.; Li, J.; Huang, Y. P.; Zhao, J. C.; Yu, J. C. *Chem. Commun.* **2003**, 80–81.
- (21) Bader, H.; Sturzenegger, V.; Hoigne, J. *Water Res.* **1988**, *22* (9), 1109–1115.
- (22) Tamura, H.; Goto, K.; Yotsuyanagi, T.; Nagayama, M. *Talanta* **1974**, *21*, 314–318.
- (23) Lin Vien, D.; Norman, C.; Grasselli, J. *Handbook of Infrared and Raman Characteristic Frequencies of Organic Molecules*; Academic Press: New York, 1991.
- (24) Bandara, J.; Mielczarski, J. A.; Kiwi, J. *Langmuir* **1999**, *15*, 7670–7679.
- (25) (a) Wu, T. X.; Li, T.; Zhao, J. C.; Hidaka, H.; Sepone, N. *Environ. Sci. Technol.* **1999**, *33*, 1379–1387. (b) Wu, T. X.; Liu, G. M.; Zhao, J. C.; Hidaka, H.; Sepone, N. *New J. Chem.* **2000**, *24*, 93–98.
- (26) Hadasch, A.; Sorokin, A.; Rabion, A.; Meunier, B. *New J. Chem.* **1998**, 45–46.
- (27) (a) Chen, K.; Costas, M.; Kim, J.; Tipton, A. K.; Que, L., Jr. *J. Am. Chem. Soc.* **2002**, *124* (12), 3026–3028. (b) Kremer, M. L. *Trans. Faraday Soc.* **1962**, *58*, 702. (c) Sawyer, D. T.; Sobkowiak, A.; Matsushita, T. *Acc. Chem. Res.* **1996**, *29*, 409–419.
- (28) (a) Gouterman, F. A. M.; Aronowitz, S. J. *Phys. Chem.* **1976**, *80*, 2184–2189. (b) Eaton, W. A.; Hochstrasser, R. M. *J. Phys. Chem.* **1968**, *46*, 985–990. (c) Balmer, M. E.; Sulzberger, B. *Environ. Sci. Technol.* **1999**, *33*, 2418–2422. (d) Maldotti, A.; Molinari, A.; Amadelli, R. *Chem. Rev.* **2002**, *102*, 3811–3836.
- (29) Sawyer, D. T.; Sobkowiak, A.; Matsushita, T. *Acc. Chem. Res.* **1996**, *29*, 409–416.
- (30) (a) Chen, K.; Que, L., Jr. *J. Am. Chem. Soc.* **2001**, *123* (26), 6327–6337. (b) Mekmouche, M.; Carole, S. M.; Marc, Fontecave, T. D.; Galey, J. B.; Lebrun, C.; Pecaut, J. *Angew. Chem., Int. Ed.* **2001**, *40* (5), 949–952.
- (31) (a) Nango, M.; Lwasaki, T.; Takeuchi, Y.; Kurono, Y.; Tokudo, J.; Oura, R. *Langmuir* **1998**, *14*, 3272–3278. (b) Nango, M.; Kimura, Y.; Ihara, Y.; Kuroki, K. *Macromolecules* **1988**, *21*, 2330–2335.